4-D quantitative GPR analyses to study the summer mass balance of a glacier: a case history

E. Forte, M. Dossi, M. Colle Fontana
University of Trieste
Department of Mathematics and Geosciences (DMG)
Trieste, Italy
eforte@units.it

R.R. Colucci
National Research Council (CNR)
Department of Earth System Sciences and Environmental Technology
(ISMAR) Trieste, Italy

Abstract— **In order to assess the seasonal changes of the topography, the inner structure and the physical properties of a small glacier in the Eastern Alps, we performed a 4-D multi frequency GPR survey by repeating the same data acquisition in four different periods of the year 2013. The usual glacier mass balance estimation encompasses only topographic variations, but the real evolution is much more complex and includes surface melting and refreezing, snow metamorphism, and basal melting. We analyzed changes in both the imaged geometrical-morphological structures and the densities, estimated from GPR data inversion. The inversion algorithm uses reflection amplitudes and traveltimes to extract the electromagnetic velocity in the interpreted layers and the densities of the frozen materials through empirical relations. The obtained results have been compared and validated with direct measures like snow thickness surveys, density logs within snow pits and ablation stakes. This study demonstrates that GPR techniques are a fast and effective tool not only for glacial qualitative studies, but also for detailed glacier monitoring and accurate quantitative analyses of crucial glaciological parameters like density distribution and water runoff.**

Keywords – glacier mass balance, 4-D GPR, GPR inversion.

I.   INTRODUCTION

Snow and ice depths and stratigraphy, along with their temporal and spatial evolution, are essential data not only for scientific glaciological purposes, but also for several practical applications like avalanche forecasting, hydrological modeling and climate change assessment. GPR techniques have been successfully applied at different scales since many years due to the overall low electric conductivity of frozen materials, which allows to reach investigation depths that would be impossible to reach in other, more common, environments [1]-[4]. In particular, GPR surveys are traditionally applied to image the ice stratigraphy, measure the snow/ice thickness and evaluate the volume of glaciers [5]-[7]. On the other hand, GPR studies focusing on time monitoring of subsurface evolution (i.e. 4-D analyses) are still challenging and, outside glaciological applications, encompass in particular fluid migration both within sediments [8]-[10] and in compact rock formations [11], [12].

As far as we know, no examples are available about the seasonal monitoring of glaciers performed by repeated GPR surveys (4-D), while there are examples related to the permafrost active layer evolution [13]. In fact, GPR is able not only to image the thickness variations due to either melting or snow accumulation, but also to highlight morphological changes within the frozen material due to snow/firn metamorphism or to local melting/refreezing phenomena. Such aspects are crucial for glaciological analyses, but densely spaced data are almost impossible to obtain with traditional techniques like snow pits, ablation stakes or even boreholes.

A glacier's mass balance (MB) describes its mass inputs and outputs over different spatial and temporal scales, providing a quantitative expression of volumetric changes through time [14]. MB is usually expressed in terms of water equivalent (WE), in units of meters of water. Mass inputs (accumulation) and mass loss (ablation) are closely related to climate and climate changes. Several different methods to determine the mass balance of ice masses exist, ranging from remote geodetic methods to direct field glaciological measurements. Geodetic methods are based on calculating the volumetric changes of an ice mass from repeated topographic surveys of surface elevation and extent (repeated aerial photographs, satellite images and lately the more precise LiDAR surveys). Glaciological methods, however, involve repeated point measurements at the glacier surface to yield rates of mass changes and, in routine monitoring programmes, are generally performed twice per year, at the end of the main principal mass balance season (in Spring and Fall). Ablation is generally measured by reference to stakes inserted into the glacier surface and fixed at that datum. The distance from the ablating snow/ice surface to a reference point is then measured repeatedly.

The use of LiDAR, especially for small ice masses, has the great advantage of detecting the entire surface of a glacier with very high accuracy and resolution. Glaciological methods allow to measure the behaviour and the evolution of a glacier only along some transects, and thus such data have to be interpolated for the entire surface. These methods have the advantage of being very cheap if compared with the LiDAR, but the disadvantage of being very time consuming. To estimate the WE, a constant density value (typically 0.90-0.92 g/cm^3) is often assumed for the entire frozen body [15]. This approximation is no longer applicable for small glaciers, which are characterized by strong density variations, with layers made of glacier ice, refrozen meltwater, firn, snow, and even debris [15]. The correct evaluation of the different densities of all the frozen components of a glacier is therefore crucial for mass

balance estimations and evolution forecasts. In this paper we apply the inversion procedure used by [16], generalization of [17], to estimate the electromagnetic (EM) velocities and subsequently the densities of frozen materials from common offset (CO) GPR data, and we critically compare the results with the ones obtained by traditional direct techniques.

II. MATERIALS AND METHODS

We selected as a test site for the 4-D monitoring a small glacier (i.e. a glacieret, in the international glaciological literature) named Prevala (North-East Italy), which can actually be considered the lowermost glacieret of the entire Alpine Chain (although not yet inserted in the Italian inventory), having minimum and maximum elevations of about 1830 and 1960 m a.s.l., respectively (Fig. 1). This is a favorable test site not only for logistical reasons, but especially because it contains different frozen materials from snow to firn and ice, and also a debris level, which represents a sort of marker horizon for both geophysical and direct measurements.

The GPR surveys were made along two intersecting profiles (Fig. 2) on June 19th 2013 (JU), i.e. soon after the beginning of the melting period, and repeated in the same year on August 6th (AG), September 4th (ST) and October 25th (OC) at the beginning of the winter season at that elevation. We used a ProEx Malå Geoscience GPR, equipped with 250, 500 and 800 MHz shielded antennas, in order to evaluate the different performances in terms of penetration depth and resolution. We further collected some common mid-point (CMP) gathers, as well as records at fixed positions with the antennas at a constant elevation equal to 1 m above the frozen surface, in order to obtain an undistorted air wave, which is essential to extract the reference amplitude used in the inversion procedure described hereafter. A DGPS device was used for trace positioning, while the GPR triggering was done by an odometer; the mean trace interval was 0.1 m. Dedicated total station measures were further acquired at some specific control points to improve the overall accuracy of the topographic survey.
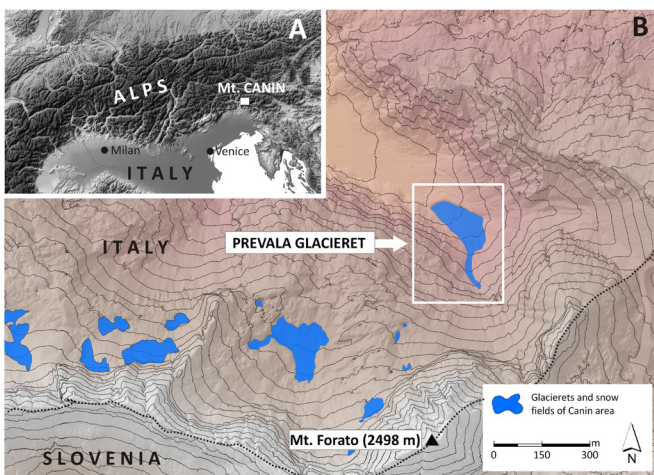

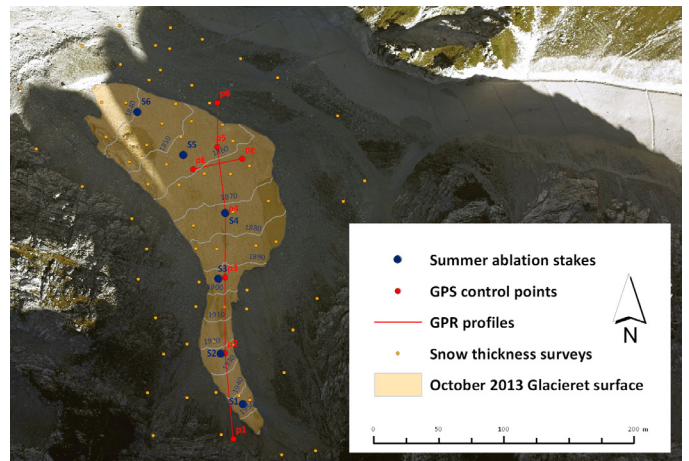Figure 1. Location map of the Prevala Glacieret, used as a test site for the 4-D GPR surveys.

Figure 2. Orthophoto with superimposed the glacieret's surface in October 2013 and the locations of the GPR surveys, the summer ablation stakes and the snow thickness surveys.

During the first GPR survey we also measured the thickness of winter snow accumulation on the glacieret by direct sampling (orange dots on Fig. 2). Then, in order to assess the seasonal melt rates in the Prevala area, we used six 2.5 m long ablation stakes inserted into the snow pack. The stakes were placed in mid-May and then clinched about every 2 weeks until October 25th, thus covering the entire 2013 melting season.

The CO data were processed using several softwares (including ProMAX - Landmark and Vista - Gedco, both originally developed for reflection seismics), with a processing flow that includes DC removal, drift removal (zero time correction), elevation (static) correction, geometrical spreading correction, time domain filtering (background removal), bandpass filtering and 2D migration (Kirchhoff). For each dataset we used a constant velocity in order to apply the spreading correction: 20.8, 20.6, 20.5 and 20.3 cm/ns for JU, AG, ST and OC, respectively. Such data have been derived from the snow densities measured within the snow pits dug close to the crossing point of the GPR profiles, and converted in EM velocities using the Looyenga's formula [18]. We checked such values considering both the diffraction hyperbola fitting on CO data and the CMP analysis. We applied a true-amplitude processing, i.e. we did not apply algorithms that may distort the trace amplitudes, like automatic gain control functions. This is actually the only way to obtain amplitudes related only to the subsurface electric impedance contrasts, i.e. to the reflection coefficients. Fig. 3 shows an example of the processing effects on the JU 250 MHz North-South profile. The sections shown in Figs. 3A and 3B are full-processed and depth converted with a preliminary constant velocity equal to 20.8 cm/ns. Since the elevation difference is more than 120 m for a profile of about 200 m in length, the topographic (static) correction makes it very difficult to represent the profile at a useful scale. Therefore, we interpreted the internal glacieret layers on time sections without any topographic correction (Fig 3C). This is possible since the inversion procedure needs, for each trace, only the two-way traveltime values with the zero time as a reference. We highlight not only the glacieret bottom (IB) and the top of an internal, laterally continuous debris layer

(TD), but also several reflectors below the debris (in different blue tones on Fig. 3C) and above it (in different yellow tones on Fig. 3C). The amplitudes/traveltimes of the latter ones have been used in the inversion procedure, while the former ones are too distorted by the highly diffractive debris.

The implemented algorithm is able to estimate, among other quantities, the thicknesses and the density distribution inside a glacier using as input: (1) the offset; (2) the EM velocity in the shallowest layer; (3) the peak amplitude of the wavelet incident on the first interface and (4) the peak amplitudes and traveltimes along each reflector. In the present case: (1) the offset was known; (2) the EM velocity in the shallowest layer was estimated by direct density measurements and assumed constant along each GPR profile; (3) the reference amplitude was the mean peak airwave amplitude recorded by the dedicated measurements; (4) the reflections were picked along the interpreted horizons, after appropriate data processing, in order to satisfy the assumptions of the inversion program. There are four approximations/assumptions necessary for the inversion procedure: (A) the propagating radar signal is an EM plane wave; (B) each layer is isotropic, homogeneous, lossless and non-dispersive; (C) in the neighbourhood of each trace position the reflectors are plane-parallel; (D) the amplitudes of the picked reflected waves are only due to partial reflections, while all the other effects are either disregarded or corrected. For each GPR trace the inversion algorithm iteratively calculates for each layer the thickness and the EM velocity (linked to the density of frozen materials through empirical relations) by reconstructing the travel paths of each reflected wave, which, with the aforementioned assumptions, are geometrically fixed and symmetric with respect to the mid-axis.
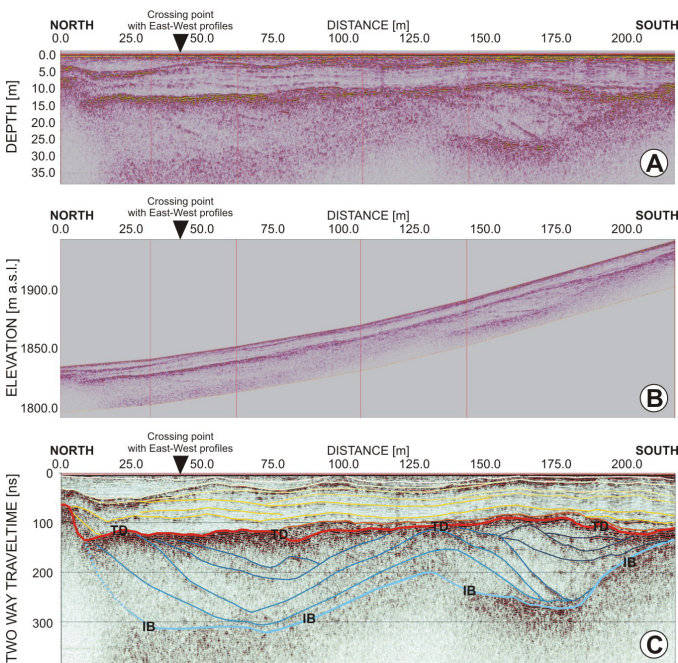
The general principle is that from the first *n-1* layer thicknesses and the EM velocities in the first *n* layers, the *n-th* cycle calculates the *n-th* layer thickness and the EM velocity in the *(n+1)-th* layer by reconstructing the travel path of the *n-th* reflected wave. Further details about the inversion procedure are available in [16], [17]. From the density distribution it is possible to estimate the WE along each profile, calculate the seasonal mass balance and highlight the stratigraphic changes using 4-D GPR profiles.

III. DATA ANALYSIS, INVERSION AND VALIDATION

By visually comparing homologous profiles acquired at different times, it is possible to observe the melting effect, which can produce strong variations of the topographic surface. This is a further problem for the 4-D analysis since we must take into account not only the subsurface time variations, but also carefully compensate for the changes of the acquisition surface. Fig. 4 shows the 500 MHz full-processed East-West profiles acquired on JU, AG, ST and OC: the topographic surface has a variation up to 8 m, while the TD shows only minor morphological changes. We can observe that in the central part of the profiles there is an absorption point, which becomes more evident with the progressive melting of the upper layers.

Fig. 5 provides the depths of TD obtained inverting amplitudes and traveltimes for the interpreted reflectors down to TD along the East-West 500 MHz profiles shown on Fig. 4. The error bars are obtained applying the propagation of maximum errors on all the inversion equations. The errors of each input parameter are: (1) zero for the offset (i.e. not considered); (2) 0.2 cm/ns for the EM velocity in the shallowest layer; (3) 5% for both reference and reflected amplitudes and (4) half of the sampling interval for the traveltimes (0.119 ns). We can notice that the lateral trend is similar for all the considered curves, showing an almost constant melting along the considered profile, while, as expected, the error bars are generally smaller for the later profiles (OC and ST), due to a lower number of reflectors. In fact, the mean uncertainties are 0.46 (JU), 0.37 (AG), 0.14 (ST) and 0.05 m (OC).

These results were compared with those obtained interpolating the snow thickness surveys (see Fig. 2). To better highlight the trends, we show in Fig. 6 the differences between the results of each period and the latter ones (OC), for both GPR (continuous lines) and interpolated direct measures (dots). The consistency of the two methodologies is apparent, while the main differences are related to greatly different data densities. In fact, GPR inversion allows to estimate the thicknesses (as well as other parameters like EM velocities, electric permittivities and densities) for each trace, taken about every 10 cm, while the snow thickness surveys have a mean sampling interval of about 20 m, which explains the smoother trends of the dots on Fig. 6. The general correspondence of the two independent estimations justifies the use of the inverted thickness and density values to calculate the WE along the GPR profiles. Fig. 7 shows the obtained results for the 500 MHz East-West profiles. As expected, the error bars are larger than the ones of the thicknesses in Fig. 5, since there is one more parameter (density) involved.

Figure 3.   GPR 250 MHz North-South profile acquired in JU. Full-processed profile without (A) and with (B) the topographic correction; C) Interpreted profile. TD: Top of the debris layer; IB: ice bottom. Toward North, at the beginning of the profile, a frontal moraine is apparent.
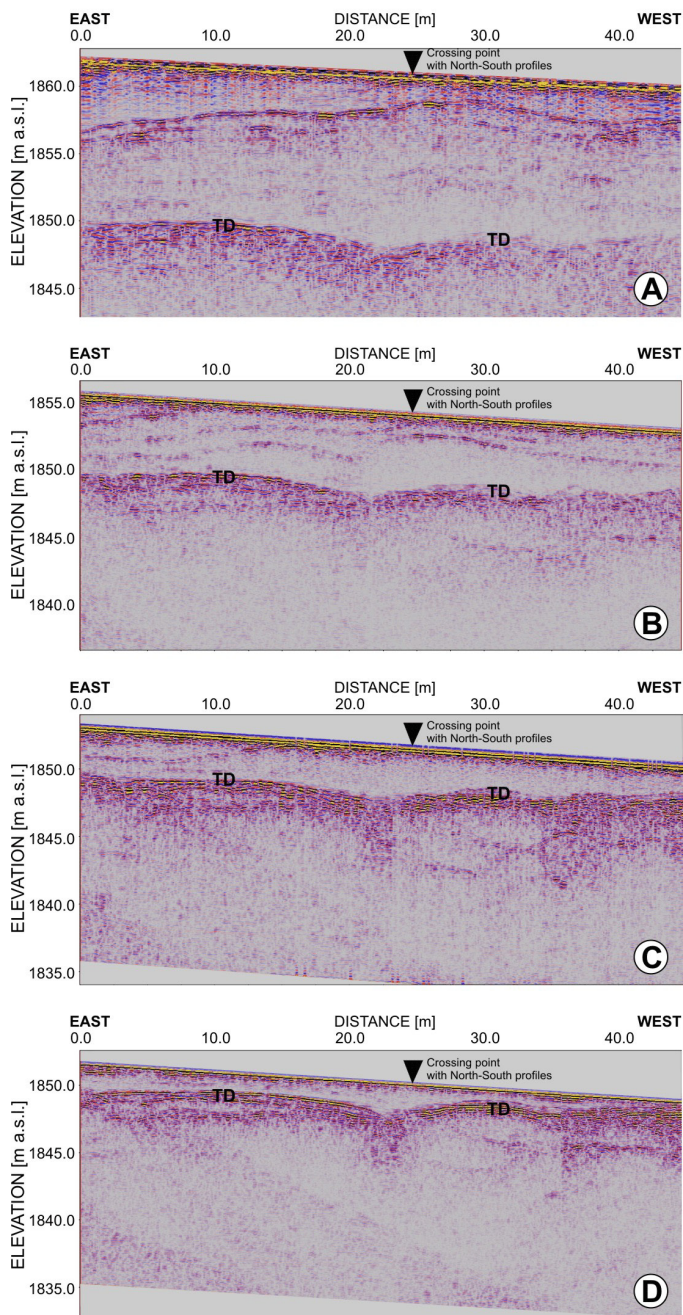
Figure 4. Comparison of 500 MHz full-processed East-West GPR profiles acquired in JU (A), AU (B), ST (C) and OC (D) 2013 across the Prevala Glacieret. TD: top of the debris.

We stress that both the thicknesses and the densities are calculated trace by trace independently, which explains possible local spikes, while the global trends are preserved. Therefore, the results can be used to describe the system on a global (tens of meters) rather than a local (tens of centimeters) scale, and the large number of available data makes the results statistically sound.
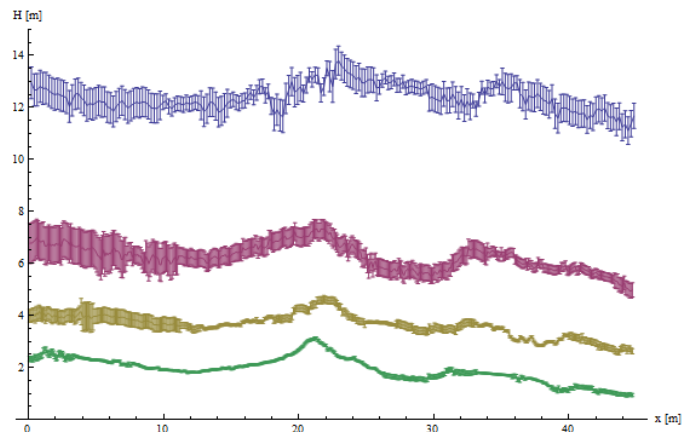
Figure 5. Thicknesses of the frozen materials estimated by GPR data of East-West 500 MHz profiles acquired (from top to bottom) in JU (blue), AG (violet), ST (brown) and OC (green) 2013. The abscissa gives the horizonthal distance from East to West.
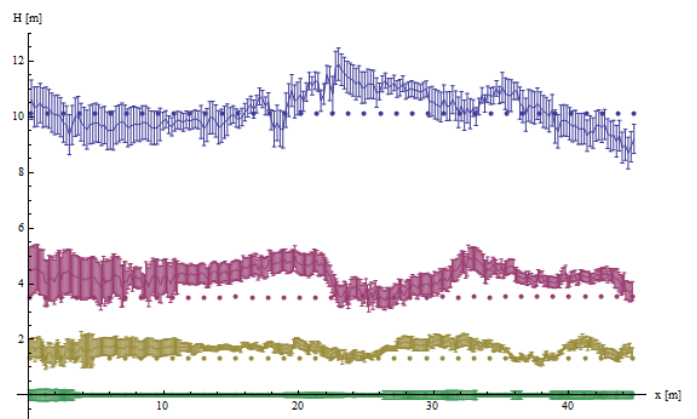

Figure 6. Comparison between the thicknesses variations of (from top to bottom) JU (blue), AG (violet), ST (brown) and OC (green), with respect to OC, for independent datasets obtained from GPR data inversion (continuous lines) and from direct measures interpolations (dots).
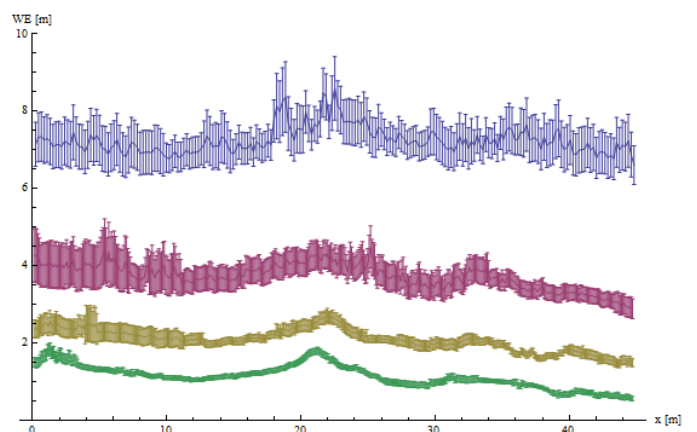

Figure 7. WE (and therefore MB) of (from top to bottom) JU (blue), AG (violet), ST (brown) and OC (green), obtained using only GPR data (East-West profiles) for the estimation of both thickness and density values.

IV. Conclusions

The previously described results demonstrate the applicability of the GPR as an efficient tool to calculate the seasonal MB of a glacier. In fact, the applied inversion procedure allows not only to define an accurate EM velocity field from a CO dataset, but also to estimate with very high resolution the densities of the frozen materials. Such data are essential to recover the total water mass stored into the glacier and its temporal variations. The 4-D experiment outcomes are therefore comparable with those obtained with traditional techniques, and are even more accurate and less time consuming. Further efforts will be addressed to the quantitative evaluation of the glaciological variations with time. Such data are essential to describe the glacial metamorphism and its behavior in different seasons, which in turn are the main parameters for short and long term evolution forecasts.

References

[1] Annan A.P., Cosway S.W., and Sigurdsson T., "GPR for snow water content", Fifth international conference on GPR. Waterloo Centre for Groundwater research, Univ. of Waterloo, Ontario, Canada, 1994, 465-475.

[2] Arcone S.A., "High resolution of glacial ice stratigraphy: a ground-penetrating radar study of Pegasus Runway", McMurdo Station, Antarctica, Geophysics 61, 1996, 1653–1663.

[3] Lundberg A., Richardson-Näslund C., and Andersson C., "Snow density variations: consequences for ground-penetrating radar", Hydrological Processes, 20, 2006, 1483–1495.

[4] Godio A., "Georadar measurements for the snow cover density", American J. of Applied Sciences, 6, (3), 2009, 414-423.

[5] Navarro F.J., Glazovsky A.F., Macheret Yu.Ya., Vasilenko E.V., Corcuera M.I., and Cuadrado M.L., "Ice-volume changes (1936–1990) and structure of Aldegondabreen, Spitsbergen", Annals of Glaciology 42, 2005, 158–162.

[6] Bælum K. and Benn D.I., "Thermal structure and drainage system of a small valley glacier (Tellbreen, Svalbard), investigated by ground penetrating radar", The Cryosphere, 5, 2011, 139–149.

[7] Singh K.K., Datt P., Sharma V., Ganju A., Mishra V.D., Parashar A., and Chauhan R., "Snow depth and snow layer interface estimation using Ground Penetrating Radar", Current Science, 100-10, 2011, 1532-1539.

[8] Brewster M.L. and Annan A.P., "Ground penetrating radar monitoring of a controlled DNAPL release: 200 MHz radar", Geophysics, 1994, 59, 1211-1221.

[9] Birken R. and Versteeg R., "Use of four-dimensional ground penetrating radar and advanced visualization methods to determine subsurface fluid migration", J. of Applied Geoph., 43, 2000, 215-226.

[10] Lopes de Castro, D. and Gomes Castelo Branco M.R, "4-D ground penetrating radar monitoring of a hydrocarbon leakage site in Fortaleza (Brazil) during its remediation process: a case history", J. of Applied Geoph., 54, 2003, 127-144.

[11] Truss S., Grasmueck M., Vega S., and Viggiano D.A., "Imaging rainfall drainage within the Miami oolitic limestone using high-resolution time-lapse Ground Penetrating Radar", Water Resources Research, 43, 3, 2007, W03405.

[12] Grasmueck M, Marchesini P., Eberli G.P., Zeller M., and Van Dam R.L., "4D GPR Tracking of Water Infiltration in Fractured High-Porosity Limestone", Extended abstracts of the 13th International Conference on Ground Penetrating Radar, Lecce, Italy, 21–25 June 2010, 1-6.

[13] Wollschläger, U., Gerhards H., Yu Q., and Roth K., "Multi-channel ground-penetrating radar to explore spatial variations in thaw depth and moisture content in the active layer of a permafrost site", The Cryosphere, 4, 2010, 269-283.

[14] Hubbard B. and Glasser N., Field techniques in Glaciology and Glacial Geomorphology, John Wiley & Sons Ltd., 2005, 400 pp.

[15] Paterson W.S.B., The physics of glaciers, 3rd edition, Elsevier Science, Tarrytown, N.Y., 1994, 480pp.

[16] Dossi M., Forte E., Pipan M., Colucci R.R., "A new methodology to estimate the EM velocity from Common Offset GPR: theory and application on synthetic and real data", Extended abstract of the 32nd GNGTS congress, Trieste, November 2013, 112-118, ISBN 978-88-902101-9-8.

[17] Forte E., Dossi M., Colucci R.R., and Pipan M., "A new fast methodology to estimate the density of frozen materials by means of common offset GPR data", Special issue of the J. of Applied Geoph.: Forward and Inverse Problems in GPR Research, 99, 2013, 135-145.

[18] Looyenga H., "Dielectric constants of heterogeneous mixtures", Physica, 31, 1965, 401-406.